Virtual roughness textures via a surface tactile texture display using vibrotactile and electrostatic friction stimuli: Improved realism

Kazuya Otake
dept. Mechanical Systems Engineering
Nagoya University
Nagoya, Japan
otake.kazuya@j.mbox.nagoya-u.ac.jp

Hikaru Hasegawa
dept. Mechanical Systems Engineering
Nagoya University
Nagoya, Japan
hasegawa.hikaru@c.mbox.nagoya-u.ac.jp

Shogo Okamoto
dept. Mechanical Systems Engineering
Nagoya University
Nagoya, Japan
okamoto-shogo@mech.nagoya-u.ac.jp

Yoji Yamada
dept. Mechanical Systems Engineering
Nagoya University
Nagoya, Japan
yamada-yoji@mech.nagoya-u.ac.jp

***Abstract*—In this study, improved realism of virtual roughness textures is verified by using vibrotactile and electrostatic friction stimuli in conjunction. Because these two types of stimuli have complementary features, they are expected to enhance the perceived quality of stimuli. In our previous research, conjunct stimuli improved the realism of virtual surfaces with sinusoidal surface roughness profiles. In this research, we tested with complicated surface roughness, and experimental participants ranked vibrotactile, electrostatic friction, and conjunct conditions in terms of realism compared to actual roughness textures. The conjunct condition was judged to be more realistic for simple and complicated surface profiles consisting of one or two spatial wave components.**

***Index Terms*—Tactile Texture Display, Vibrotactile Stimuli, Electrostatic Friction Stimuli**

I. Introduction

According to the spread of touch-panel interfaces, expectations for tactile texture feedback technology have been increasing. Tactile texture displays suitable for touch panels are mainly vibrotactile types [1], [2], [3], [4] and friction-variable types [5], [6], [7], [8], [9]. The former type involves driving the panel mechanically and deforming a finger pad by touching the panel. The latter type entails controlling friction on the panel. Many tactile displays that were previously studied were based on one of these two types of tactile stimulus, whereas a few perceptual studies about the conjunct vibrotactile and electrostatic friction stimuli were reported [10].

Because tactile perception of surfaces is expressed in a multidimensional information space [11], tactile texture displays presenting multiple haptic modalities are effective methods to present texture [1], [12], [13]. These studies entailed combining multiple tactile stimuli to improve the realism of virtual textures. However, there is little research on the effects of using multiple tactile stimuli together via tactile texture displays implementing touch panels.

In this research, we investigated the effects of combining vibrotactile and electrostatic friction stimuli to present virtual texture surfaces in terms of realism. In principle, using vibrotactile stimuli is an appropriate method for presenting surface textures [1], [3]. Use of electrostatic friction stimuli involves presenting texture using the spatial distribution of friction and vibration caused by friction [5], [6], [7]. These two types of stimuli are efficient to present surface roughness and friction characteristics, respectively. Hence, the use of vibrotactile and frictional stimuli in conjunction widens the texture space to be covered. However, thus far only limited studies have been reported [14], [15].

Our previous research indicated the effects of combining vibrotactile and electrostatic friction stimuli in terms of presenting virtual roughness with sinusoidal surface profiles [14], [15]. In this study, we investigated the same effects as in previous studies in cases of more complicated texture surfaces. We adopted surfaces that were three-dimensionally printed (3D-printed) by synthesizing two sinusoidal waves with different wavelengths and natural materials such as cloth and wood as complicated texture surfaces.

II. Principles of vibrotactile and electrostatic friction display

In this study, we focused on the effect of using two principles of tactile stimuli that possess complementary features.

978-1-7281-7392-4/20/$31.00 ©2020 IEEE

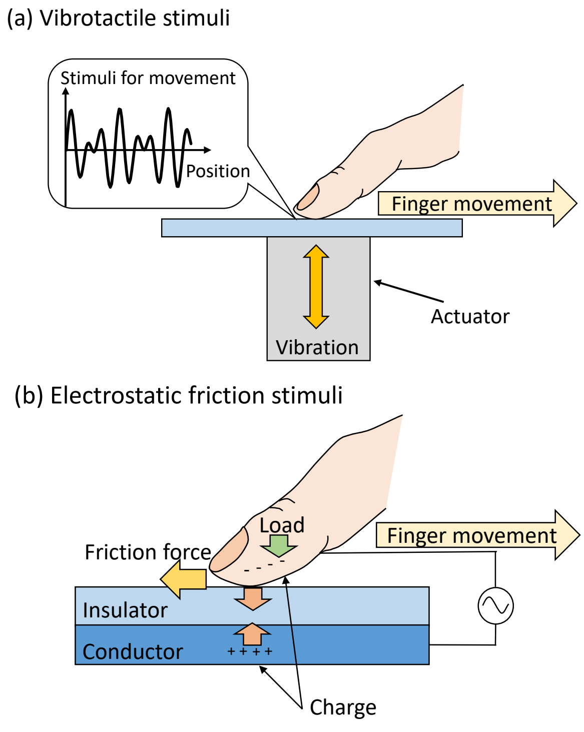

Fig. 1. Principles of (a) vibrotactile and (b) electrostatic friction stimuli.

A. Vibrotactile display

Vibrotactile stimuli drive the panel using an actuator, as shown in Fig. 1(a), deforming a finger pad. Such tactile stimuli are presented in the normal direction in the present study. Surface roughness textures can be presented by producing vibrotactile stimuli pertaining to surface displacement [1], [2], [3], [4]. Because the touch panel itself actively produces mechanical stimulation, this display does not necessarily need active finger movement. However, tactile stimuli synchronized with finger movement are known to be effective method for presenting stimuli.

B. Electrostatic friction display

Electrostatic friction stimuli control the electrostatic attractive force generated by applying a voltage between the finger pad and the panel, as shown in Fig. 1(b). The attractive force increases the friction between the finger and panel. The finger pad is then deformed along the shear direction by the friction force when the finger slides across the panel. Such stimuli are efficient in presenting surface texture dominated by the friction force [6], [7]. A display of this type does not need a mechanical drive, thereby simplifying its implementation. However, the strength of the perceived friction stimuli depends on the individual, because of the dielectric constant of the finger pad.

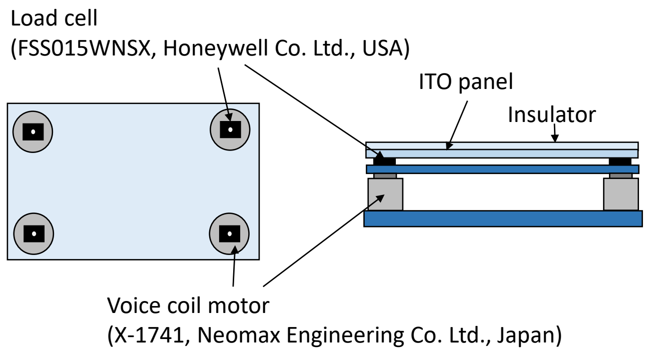

Fig. 2. Schematic view of the tactile texture display used in the experiment.

III. Apparatus: Tactile Texture Display Using Vibrotactile and Electrostatic Friction Stimuli

In this experiment, we used a tactile texture display presenting vibrotactile and electrostatic friction stimuli simultaneously (Fig. 2). There are few tactile displays that can output both types of stimuli at the same time. This display was used in our previous research [14], [15] where electrostatic friction stimuli were presented via a conductive pad to control friction. In contrast, stimuli are presented to the finger pad directly in the current study.

Vibrotactile stimuli were generated by voice coil motors (X-1741, Neomax Engineering Co., Ltd., Japan) located in the four corners below the panel. These four actuators were driven synchronously by an audio amplifier (FX-AUDIO-FX-502J, North Flat Japan Co., Ltd., Japan) and presented a displacement normal to the panel. This setup can present suprathreshold vibrations at up to at least 300 Hz.

Electrostatic friction stimuli were produced by applying a voltage between the finger pad and the indium tin oxide (ITO) panel with an insulator film attached. The stimuli were experienced by touching the panel while holding a stainless bar connected to ground. The applied voltage was amplitude modulated over a carrier frequency of 20 kHz. The modulated voltage signal was amplified by a voltage amplifier (HJOPS-1B20, Matsusada Precision Inc., Japan), whose maximum output was ± 1 kV, with a response of 75 kHz.

Four load cells (FSS015WNSX, Honeywell Co., Ltd., USA) were placed between the panel and the actuators. Finger position was measured by the output ratio of these load cells. Tactile stimuli were controlled for finger movement.

Two voltage amplifiers for the two types of stimuli and load cells were connected to a computer via a data acquisition board (TNS-6812, Interface Co., Ltd., Japan). The sampling frequency was determined to be $\sim$667 Hz.

IV. Experiment: Comparison of Realism among Stimuli Conditions

We verified that the realism of the virtual roughness texture is improved by using vibrotactile and electrostatic friction stimuli in conjunction. We created a virtual texture that imitates roughness texture with one or two spatial frequency components and natural materials.

A. Ranking task

Participants experienced texture stimuli under the following conditions: only vibrotactile stimuli were presented, only electrostatic friction stimuli were presented, and both stimuli were presented. The participants ranked the three stimuli conditions in terms of realism, and then determined the most realistic stimuli condition. They were instructed to trace the virtual and real surfaces at the same finger speed and strength for roughness textures or natural materials to compare them. They were allowed to experience virtual stimuli and actual stimuli any number of times in each trial. One trial was conducted for each roughness texture and each natural material. They washed their hands and removed extra moisture or oil on their fingertips before the experiment. The panel was lubricated by talcum powder to reduce the effect of friction in the experiment.

B. Participants

Thirteen university students (males in their 20s) participated in this experiment. Seven of these took part in the experiment on roughness textures (one or two spatial frequency components). Another six participated in the experiment on natural materials. None of the students were informed about the objective of the research.

C. Roughness textures and natural materials

Images of roughness textures and natural materials used in this experiment are shown in Fig. 3.

Table I lists the characteristics of the five actual roughness surfaces used. Three of these are surface roughness textures created by synthesizing two sinusoidal waves with different spatial wavelengths. Two other kinds are roughness textures with sinusoidal surface profiles, and these surface types were used in our previous studies [14], [15]. Listed in the table are spatial wavelength λ and peak-to-peak amplitude h values of the roughness textures. For synthesizing two different spatial wavelengths of sinusoidal waves, their phase differences were set to 0. We prepared 3D-printed actual stimuli for these roughness textures by using Form2 (Formlabs., Ltd., MA, nominal resolution: 140 μm). Our previous researches [14], [15] concluded that for relatively large spatial wavelengths (1.0 mm$\leq \lambda \leq$3.0 mm), vibrotactile stimuli with slight electrostatic friction stimuli were effective for presenting virtual sinusoidal surfaces. Therefore, we investigated the effectiveness of conjunct stimuli in this range. Wood, cork, drawing paper, and denim were used as natural materials, as they are considered commonly touched surfaces.

D. Virtual roughness textures

Roughness textures were presented by using vibrotactile and electrostatic friction stimuli. We used a tactile stimulation algorithm to deform a finger pad based on the relationship between finger movement and surface displacement [3].

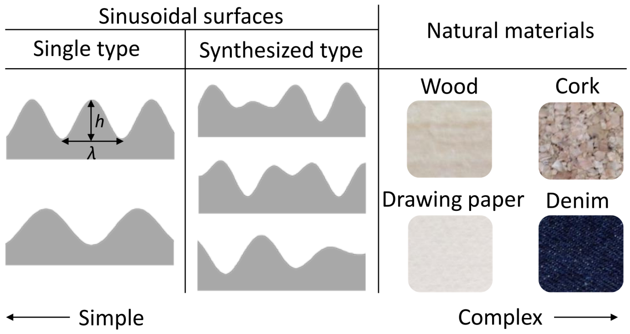

Fig. 3. Images of roughness textures and natural materials.

TABLE I
SPATIAL WAVELENGTH λ AND PEAK-TO-PEAK AMPLITUDE h VALUES OF ROUGHNESS TEXTURES.

Sinusoidal surface	λ_1 (mm)	λ_2 (mm)	h (mm)
Single type	1.5	—	1.0
	2.5	—	1.0
Synthesized type	1.3	1.9	1.2
	1.3	2.5	1.2
	1.9	2.5	1.2

1) Vibrotactile stimuli simulating roughness textures: To simulate skin vibration generated by tracing surfaces of the roughness textures, the driving force of the voice coil motors was set to

$$F_v(t) = A \sin\left(2\pi \frac{x(t)}{\lambda_1}\right) + B \sin\left(2\pi \frac{x(t)}{\lambda_2}\right), \quad (1)$$

where A, B, and $x(t)$ are the gains for each sinusoidal wave and the finger position on the touch panel at time t, respectively, and λ_1 and λ_2 express spatial wavelengths for each sinusoidal wave. Similar formulas were used in previous researches [4], [6], [7]. λ values were determined as listed in Table I. In case of presenting roughness textures with single sinusoidal surface profiles, the driving force $F_v(t)$ was determined by using only the first term on the right side of (1).

2) Electrostatic friction stimuli simulating roughness textures: Based on the electrostatic force law and Coulomb's law of friction, the relationship between the shear force $F_e(t)$ and the applied voltage $V_e(t)$ generated by tracing the panel is described as

$$F_e(t) = \mu\{W + kV_e(t)^2\}, \quad (2)$$

where μ, W, and k are the coefficient of friction on the panel, the normal load of the finger, and a constant of the electrostatic friction force, respectively. The shear force generated by sliding across an uneven surface with a finger is a gradient function of the surface displacement [16], [17]. This means that the shear force phase deviates by $\pi/2$ from that of surface displacement. Therefore, the applied voltage was set so that $F_e(t)$ was generated as

$$F_e(t) = \mu \left[W + k \left\{ C \cos\left(2\pi \frac{x(t)}{\lambda_1}\right) + D \cos\left(2\pi \frac{x(t)}{\lambda_2}\right) + C + D \right\} \right], \tag{3}$$

where C and D are the gains for sinusoidal waves. The applied voltage $V_e(t)$ is presented as follows:

$$V_e(t) = \pm \sqrt{C \cos\left(2\pi \frac{x(t)}{\lambda_1}\right) + D \cos\left(2\pi \frac{x(t)}{\lambda_2}\right) + C + D}. \tag{4}$$

A similar formula was used in a previous study [7], which can be used regardless of the number of sinusoidal waves to be synthesized. For roughness textures consisting of a single sinusoidal surface profile, the applied voltage $V_e(t)$ was determined by using only the first and third terms of (4).

3) Perceived strength of virtual roughness texture: The strengths of tactile stimuli (A, B, C, and D) were determined to the value such that the synthesized stimuli were felt to be close to the sense of real roughness textures by using the method of adjustment. At this time, three stimuli conditions (vibrotactile stimuli only, electrostatic friction stimuli only, and conjunct stimuli) were adjusted to have the same perceived strength.

E. Virtual material textures

We measured the normal and shear forces generated when tracing natural materials with a finger [18]. The measured normal forces correspond to the vibrotactile stimuli that are normal to the panel for our tactile display. The shear forces correspond to the friction stimuli for our tactile display. Hence, we converted the measured normal and shear forces to vibrotactile and electrostatic friction stimuli, respectively. We used the force components above 15 Hz when the finger's normal load and speed were 1 ± 0.3 N and 70–90 mm/s, respectively. For each of the four types of natural materials, force signals lasting 500 ms were prepared. In the latter experiment, the 500-ms signal was repeatedly presented to form an endless texture.

1) Vibrotactile stimuli simulated natural materials: To present vibration components generated by tracing surfaces of the natural materials, the driving force $F_v(t)$ of voice coil motors was determined as

$$F_v(t) = \alpha f_n^i(t), \tag{5}$$

where α and $f_n^i(t)$ are gain and normal force generated by sliding material i, respectively.

2) Electrostatic friction stimuli simulated natural materials: Taking the relationship between the applied voltage and the shear force produced during tracing panel (2) into account, the applied voltage $V_e(t)$ was determined to be

$$V_e(t) = \pm \beta \sqrt{f_s^i(t) + \gamma \frac{\mu^i}{\mu_{min}}}, \tag{6}$$

where β and $f_s^i(t)$ are the voltage gain and the vibration signal of the shear force generated by tracing natural material i, respectively; μ^i is the friction coefficient of natural material i; μ_{min} is the minimum friction coefficient in those of four materials; and γ is the minimum positive value that satisfies $f_s^i(t) + \gamma \geq 0$ for all of the materials. The magnitude of DC component was determined by using the friction coefficient. μ^i was normalized by μ_{min} so that the square root of (6) was not negative, i.e., $\mu^i/\mu_{min} \geq 1$. As in Section IV-D2, the voltage determined by (6) was amplitude-modulated with the carrier frequency of 20 kHz.

3) Perceived strength of virtual material textures: The strength of tactile stimuli (given by α and β) was adjusted by participants before the ranking task. Essentially, this should match the magnitude of the measured contact force. However, this adjustment is difficult because it is influenced by the conditions of the participant's finger. In this research, α and β were adjusted so that participants could feel that the virtual material and the corresponding real natural material were similar. For the conjunct stimuli, α and β were reduced by 1 JND (Just Noticeable Difference), because conjunct stimuli tend to be perceived as stronger than either single stimuli.

V. Results

Fig. 4 shows the results of the ranking task. Figs. 4(a), 4(b), and 4(c) show the results of collective analysis of two kinds of roughness textures with sinusoidal surface profiles, three kinds of roughness textures created by synthesizing two sinusoidal waves with different spatial wavelengths, and four kinds of natural materials, respectively. The horizontal axis shows the three types of stimuli conditions, and the vertical axis shows the order of realism. The percentage of which the rank was selected is written in each grid. The higher the percentage, the darker the color in the grid; the lower the percentage, the lighter the color.

We analyzed whether there were significant differences among the ranks of stimuli conditions by using a Wilcoxon rank-sum test with a corrected p value. Significance level was set as $p < 0.05$. As shown in Fig. 4(a), the case of conjunct stimuli was selected as significantly higher than that of vibrotactile stimuli for roughness textures with sinusoidal surface profiles. This indicates that conjunct stimuli were judged more realistic than vibrotactile stimuli only.

As shown in Fig. 4(b), the case of conjunct stimuli was selected as significantly higher than each vibrotactile and electrostatic friction stimuli only for roughness textures created by synthesizing two sinusoidal waves. Hence, conjunct stimuli were judged the most realistic of the three conditions.

As shown in Fig. 4(c), no significant difference was confirmed among the three stimuli in natural materials. By material, the case of conjunct stimuli was often selected as of first rank for cork and drawing paper. In contrast, no substantial difference was observed among the three stimuli for wood and denim.

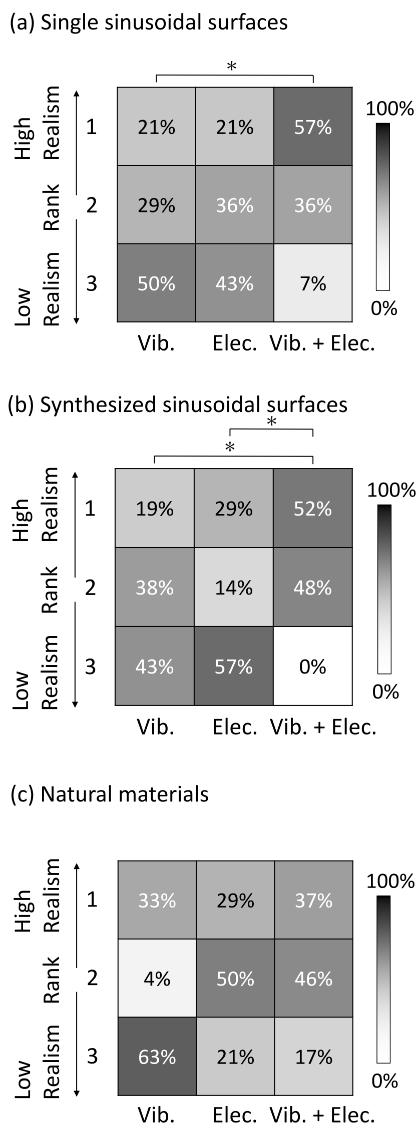

Fig. 4. Ranks of each type of surface. $*$ indicates $p < 0.05$.

VI. Discussion

We expected that using vibrotactile and electrostatic friction stimuli would have an effect in terms of presenting various virtual roughness textures. This was confirmed in presenting virtual textures imitating roughness textures with one or two spatial frequency components; however, it was not observed in presenting virtual material textures.

It may be necessary to represent both the surface displacement and the spatial distribution of friction by stimuli for presenting relative macro roughness with spatial wavelengths of $\geq$1 mm. This is why combining two kinds of stimuli contributed to improving the realism of virtual roughness textures. The superiority of conjunct stimuli was also confirmed for presenting more complicated roughness textures made by synthesizing two sinusoidal waves with different spatial wavelengths. Combining the two kinds of tactile stimuli is also an effective method for presenting complex roughness textures to some extent. In addition, it may be difficult to present virtual roughness textures by electrostatic friction stimuli only in complicated surfaces.

The superiority of conjunct stimuli was not observed in the case of presenting virtual material textures. This may be because effective stimuli conditions depend on the kind of natural material. Moreover, this result may be influenced by the algorithm used for producing the virtual stimuli and the method of adjusting their intensity.

VII. Conclusion

We investigated whether the realism of virtual roughness textures was improved by using vibrotactile and electrostatic friction stimuli in conjunction. A positive effect was confirmed for complicated roughness textures made by synthesizing two sinusoidal surfaces; however, this was not the case for stimuli made from natural textures. Our results are not conclusive for natural textures because the method for presenting such textures has not been established in the community.

Acknowledgments

This study was in part supported by MEXT KAKENHI (#17H04697 and #15H05923).

References

[1] H. Culbertson and K. J. Kuchenbecker, "Importance of matching physical friction, hardness, and texture in creating realistic haptic virtual surfaces," *IEEE Transactions on Haptics*, vol. 10, no. 1, pp. 63–74, 2017.

[2] M. Wiertlewski, J. Lozada, and V. Hayward, "The spatial spectrum of tangential skin displacement can encode tactual texture," *IEEE Transactions on Robotics*, vol. 27, no. 3, pp. 461–472, 2011.

[3] S. Asano, S. Okamoto, Y. Matsuura, and Y. Yamada, "Toward quality texture display: vibrotactile stimuli to modify material roughness sensations," *Advanced Robotics*, vol. 28, no. 16, pp. 1079–1089, 2014.

[4] S. Asano, S. Okamoto, and Y. Yamada, "Vibrotactile stimulation to increase and decrease texture roughness," *IEEE Transactions on Human-machine Systems*, vol. 45, no. 3, pp. 393–398, 2015.

[5] O. Bau, I. Poupyrev, A. Israr, and C. Harrison, "Teslatouch: Electrovibration for touch surfaces," *Proceedings of Annual ACM Symposium on User Interface Software and Technology*, pp. 283–292, 2010.

[6] Y. Vardar, A. Isleyen, M. K. Saleem, and C. Basdogan, "Roughness perception of virtual textures displayed by electrovibration on touch screens," *IEEE World Haptics Conference*, pp. 263–268, 2017.

[7] T. Fielder and Y. Vardar, "A novel texture rendering approach for electrostatic displays," *Proceedings of International Workshop on Haptic and Audio Interaction Design*, no. hal-02011782v3, 2019.

[8] T. Nakamura and A. Yamamoto, "A multi-user surface visuo-haptic display using electrostatic friction modulation and capacitive-type position sensing," *IEEE Transactions on Haptics*, vol. 9, no. 3, pp. 311–322, 2016.

[9] J. Jiao, D. Wang, Y. Zhang, D. Cao, Y. Visell, X. Guo, and X. Sun, "Detection and discrimination thresholds for haptic gratings on electrostatic tactile displays," *IEEE Transactions on Haptics*, vol. 12, no. 1, pp. 34–42, 2019.

[10] S. Ryu, D. Pyo, S.-C. Lim, and D.-S. Kwon, "Mechanical vibration influences the perception of electrovibration," *Scientific Reports*, no. 3, 2018.

[11] S. Okamoto, H. Nagano, and Y. Yamada, "Psychophysical dimensions of tactile perception of textures," *IEEE Transactions on Haptics*, vol. 6, no. 1, pp. 81–93, 2013.

[12] M. Strese, R. Hassen, A. Noll, and E. Steinbach, “A tactile computer mouse for the display of surface material properties,” *IEEE Transactions on Haptics*, vol. 12, no. 1, pp. 18–33, 2019.

[13] T. Yamauchi, S. Okamoto, M. Konyo, Y. Hidaka, T. Maeno, and S. Tadokoro, “Real-time remote transmission of multiple tactile properties through master-slave robot system,” *Proceedings of IEEE International Conference on Robotics and Automation*, pp. 1753–1760, 2010.

[14] K. Ito, S. Okamoto, H. Elfekey, H. Kajimoto, and Y. Yamada, “A texture display using vibrotactile and electrostatic friction stimuli surpasses one based on either type of stimulus,” *Proceedings of IEEE International Conference on Systems, Man, and Cybernetics*, pp. 2343–2348, 2017.

[15] K. Ito, S. Okamoto, Y. Yamada, and H. Kajimoto, “Tactile texture display with vibrotactile and electrostatic friction stimuli mixed at appropriate ratio presents better roughness textures,” *ACM Transactions on Applied Perception*, vol. 16, no. 4, 2019.

[16] Y. Fujii, S. Okamoto, and Y. Yamada, “Friction model of fingertip sliding over wavy surface for friction-variable tactile feedback panel,” *Advanced Robotics*, vol. 30, no. 20, pp. 1341–1353, 2016.

[17] G. Robles-De-La-Torre and V. Hayward, “Force can overcome object geometry in the perception of shape through active touch,” *Nature*, vol. 412, pp. 445–448, 2001.

[18] H. Hasegawa, S. Okamoto, and Y. Yamada, “Phase difference between normal and shear forces during tactile exploration represents textural features,” *IEEE Transactions on Haptics*, vol. 13, no. 1, pp. 11–17, 2020.